Surface segregation in $Mo_{0.75}Re_{0.25}(001)$ studied by low-energy alkali-ion scattering

S. H. Overbury
Oak Ridge National Laboratory, Oak Ridge, Tennessee 37831-6201

R. J. A. van den Oetelaar
Department of Physics, Eindhoven University of Technology, 5600 MB Eindhoven, The Netherlands

D. M. Zehner
Oak Ridge National Laboratory, Oak Ridge, Tennessee 37831-6057
(Received 30 November 1992)

$Mo_{0.75}Re_{0.25}(001)$ has been studied by low-energy alkali-ion scattering. Using a method based upon analysis of ion-scattering intensity ratios, the Re atom fractions in the first and second layers of this surface have been determined to be 0.040 ± 0.005 and 0.52 ± 0.05, respectively. From analysis of the critical edges the first interlayer spacing is found to be contracted by about 9%. These results are in excellent agreement with recent low-energy-electron-diffraction experiments. The results are described in terms of various theories of surface segregation, and are found to be in quite good agreement with the simplest models if the surface coordination is adjusted to that associated with a smoother, higher coordination surface.

I. INTRODUCTION

Recently, low-energy-electron-diffraction (LEED) studies of binary alloy, single-crystal surfaces have demonstrated the ability to determine interlayer spacings and layer compositions for several layers depth. Studies have been carried out on Pt-Ni (Ref. 1) and Mo-Re (Ref. 2) alloy single-crystal surfaces. With this depth profiling of an equilibrated surface, interesting phenomena have been found such as a reversal of the segregating component between two different crystal faces, layer compositions and interlayer spacings which oscillate with depth, and the unproven possibility of metastable alloy surface concentrations.[3,4] A LEED study of $Mo_{0.85}Re_{0.15}(001)$ has determined layer compositions down to five layers and the top eight interlayer spacings, and studies of $Mo_{0.75}Re_{0.25}(001)$ similarly have determined six layer compositions and eight interlayer spacings.[2] Such results obviously provide a demanding test of theories attempting to predict structure and composition profiles at alloy surfaces.[3-5] Critics may argue that the determination of so many structural parameters from a LEED study requires verification by independent techniques. Medium-energy ion-scattering studies of $Pt_{0.5}Ni_{0.5}(111)$ have substantiated the basic oscillatory depth profile although the deviations from bulk composition in each layer were slightly less than obtained by LEED.[6] In this paper, the results of a low-energy alkali-ion-scattering study of $Mo_{0.75}Re_{0.25}(001)$ are reported which quantitatively confirm the first- and second-layer compositions found by the LEED study, and we find a first-layer contraction comparable to the LEED result.

II. EXPERIMENT

The $Mo_{0.75}Re_{0.25}$ alloy was grown by the crystal-growth group in the Solid-State Division at Oak Ridge National Laboratory and was cut and polished to a (001) plane to within 0.5° as determined by Laue backscattering. The sample had been used and extensively cleaned in previous examinations.[2] For the present study it was suspended in 0.25-mm W wires allowing rapid heating by electron bombardment. The sample was cleaned in UHV by high-temperature annealing in oxygen to remove surface and near-surface carbon impurities, followed by anneals to 2000 K to remove surface oxygen. This procedure, involving no ion sputtering, gave a surface which was free of carbon and oxygen as detectable by Auger electron spectroscopy (AES).

Ion-scattering measurements were performed with the apparatus used in previous studies.[7] The incident Li^+ ion beam is well collimated, monoenergetic, and mass selected. The polar angle of incidence ψ (calibrated from the macroscopic plane of the surface by laser alignment) and the azimuthal angle of incident ϕ (as determined by azimuthal scans) are variable under computer control and accurately repositionable. The scattered ions were energy analyzed by a spherical electrostatic analyzer (ESA) with a resolution of 2%, which is rotatable to allow total laboratory scattering angles θ from 0° to 135°. The accuracies of ψ, ϕ, and θ are $\pm0.5°$, 1°, and 2°, respectively.

III. RESULTS

Energy distributions of Li^+ ions scattered from the clean and annealed $Mo_{0.75}Re_{0.25}(001)$ are shown in Fig. 1 for three different incident angle conditions. The spectrum labeled *c* is for the incidence along a [110] azimuth and $\psi=40°$. At this condition scattering from first-layer atoms is possible but most single scattering from deeper layers should be shadowed. A prominent peak due to single scattering from Mo is seen at $E/E_i=0.77$, but only a weak peak due to single scattering from Re is present at higher energies. Curve *a* is also measured in the [110] az-

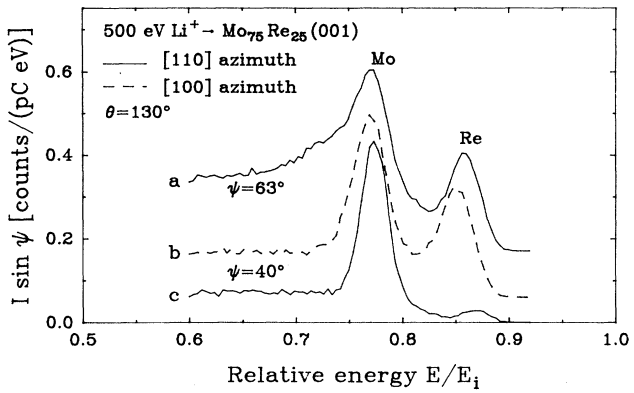

FIG. 1. Energy distributions are shown for three different incident conditions. The distributions are corrected for the energy-dependent transmission of the ESA and are multiplied by $\sin\psi$. They are also normalized to the same Mo peak height (scaling factors of 0.43 and 0.6 for $\psi=63°$ and the [100] azimuth, respectively) and are offset for clarity.

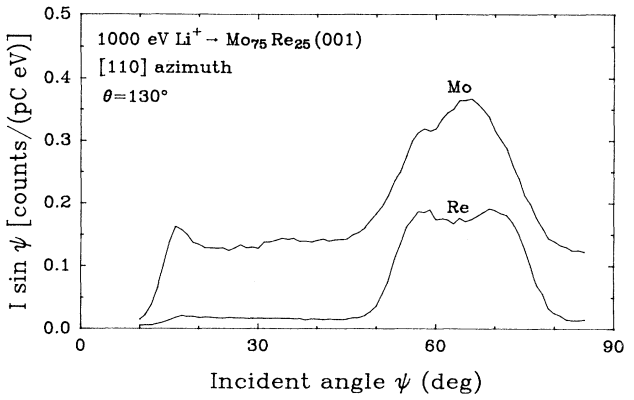

FIG. 3. Scans of the Mo and Re peak heights (corrected for ESA transmission and multiplied by $\sin\psi$) are shown as a function of incident angle in the [110] azimuth.

imuth but at a higher incident angle of 63° where second-layer atoms have emerged from shadow cones of first-layer atoms. It is seen that single scattering from Re atoms is greatly increased compared to the more grazing angle, giving rise to a pronounced peak at $E/E_i=0.86$. This observation immediately suggests that Re is depleted from the first layer compared to the second layer. Additional information is obtained from scattering along the [100] azimuth (curve *b*). In this azimuth the second-layer termination is not shadowed by the first layer at any incident angle and scattering from second-layer atoms should be possible at grazing angles (see Fig. 2). This was found to be the case as indicated by the increased intensity of both the Mo and Re peaks. The presence of a strong Re peak at $\psi=40°$ and at lower angles (not shown) supports the presence of substantial quantities of Re in either the first or second layer.

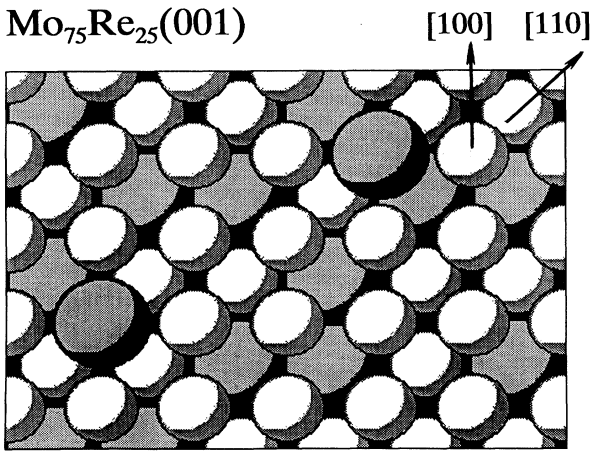

FIG. 2. A ball model shows the $Mo_{0.75}Re_{0.25}(001)$ surface. Re atoms, the darker atoms in each layer, are placed to reflect their random substitution and the measured first- and second-layer compositions.

These effects are further illustrated from incident angle scans shown in Fig. 3. These scans were obtained by setting the ESA energy at the energy of the single-scattering peak and measuring the count rate as a function of incident angle ψ. The intensities are multiplied by $\sin\psi$ to compensate for geometric foreshortening. Curves are shown for both the Mo and Re peaks in the [110] azimuth. The critical onset of scattering from first-layer atoms occurs at about 16°. Above this angle a region of nearly constant intensity occurs up to about 50° where the onset of second-layer scattering occurs. Blocking of this scattering occurs above about 72° causing a decrease in intensity back to the level characteristic of scattering from the first layer only.

The angular scans support the conclusions obtained from the energy distributions shown in Fig. 1. The data are shown for an incident ion energy of 1000 eV, but scans obtained at 500 and 2000 eV were very similar except for predictable shifts in critical edges. The constant low Re intensity at between 20° and 50° compared to the Mo intensity in the same region suggests a low concentration of Re in the first layer, while the large increase in the Re signal around 55° indicates substantial amounts of Re in the second layer. The sharp critical edges observed in the angular scans are consistent with a well-ordered surface and are located at angles consistent with the surface structure illustrated in Fig. 2.

A. Surface composition

Using data such as those shown in Figs. 1 and 3, it was possible to obtain quantitative values of the composition of the first and second layers of the $Mo_{0.75}Re_{0.25}(001)$ surface. In order to do this it is first necessary to determine the relative single-scattering cross sections for scattering from Mo compared to Re atoms.

As has been done previously,[7,8] information about scattering potentials was obtained from measurement of the location of low-angle critical edges observed in the incident angle dependence, such as shown in Fig. 3. Since the first layer has a very low concentration of Re (as dis-

cussed qualitatively above and shown below) the position of the Mo single-scattering edge in the [110] azimuth is dominated by shadowing of Mo target atoms by other Mo atoms and can thus be used to determine the Li^+/Mo scattering potential. The position of this edge (measured at the 90% point) was measured for four different scattering angles (90°, 110°, 130°, and 135°) at 500 eV and fit to the critical angles calculated for a Thomas-Fermi-Moliere (TFM) scattering potential with adjustable screening length. A value for the screening length a of $0.87a_F$ was obtained. This value is in close agreement with the value determined previously for a Mo(001) surface to be about $0.90a_F$.[8] The critical angles were also fit to within ±0.2° by the parameter-free potential suggested by Ziegler, Biersack, and Littmark (ZBL).[8,9] A measurement of the screening length for Li^+/Re could not be obtained since no conditions could be found in which Re could be isolated as the shadowing atom. For this interaction it was assumed that the ZBL potential would accurately predict the critical angles and the scattering cross sections. This potential is found to work well for W, which differs from Re by only one atomic number.[10] Calculations show that a ZBL potential gives the same critical angles (within ±0.5°) for [100] and [110] atom rows as a TFM potential with screening length $a=0.94a_F$, and so for convenience this potential could be used.

Using these forms of the scattering potential the single-scattering cross sections for Li^+ scattering from Mo and Re could be computed. A program written to compute these cross sections was checked (for the TFM potential) against the published tables of Robinson,[11] and was found to reproduce those cross sections to better than 0.1% throughout the relevant range of energy and impact parameters. The cross-section ratios are shown in the final column of Table I and should be accurate to within 10%.

Determination of the composition of the first and second layers was done using a multiparameter model of the scattering intensities. Mo and Re single-scattering intensities were measured for the three different incident angles shown in Fig. 1 yielding six intensities or five independent intensity ratios. For ψ near 40° in the [110] azimuth all scattering at the single-scattering energy is assumed to originate from the first layer. The ratio of the Mo to Re single-scattering intensities R_1 is then related to the first-layer Re atom fraction, x_1 by Eq. (1a):

$$R_1=I_{\mathrm{Mo}}/I_{\mathrm{Re}}=[(1-x_1)/x_1](s_{\mathrm{Mo}}/s_{\mathrm{Re}})\ . \tag{1a}$$

This equation alone is sufficient to give the first-layer

TABLE I. Measured ion-scattering intensity R_i, defined by Eq. (1) in the text, are given for various incident ion energies and laboratory scattering angles, both with and without background subtraction. The values of the resulting fitting parameters [from Eq. (1)] are given in the second half of the table.

		Measured ratios					
E (eV)	θ (deg)	R_1	R_2	R_3	R_4	R_5	$s_{\mathrm{Mo}}/s_{\mathrm{Re}}$[a]
			No background correction				
500	135	14.4	2.33	18.9	1.68	14.2	0.647
500	130	14.8±0.5	2.24±0.07	16.8±2.4	1.64±0.04	14.2±1.6	0.649
500	110	17.0±0.6			1.72±0.05	23.7±3.6	0.662
1000	130	14±1.5	2.72±0.08	17.5±2.0	1.59±0.03	11.8±1.0	0.615
1000	110	12.3±0.9			1.74±0.06	11.3 ±1.2	0.623
			With integral background removal				
500	135	16.3	1.86	19.1	1.43	17.3	0.647
500	130	16.3±0.7	1.84±0.06	16.8±2.4	1.41±0.04	14.1±1.6	0.649
500	110	20.9±2.2			1.65±0.05	30.3±5.8	0.662
1000	130	17.1±1.9	2.09±0.07	20.1±2.3	1.37±0.07	14.2±1.2	0.615
1000	110	16.5±2.5			1.46±0.05	14.0±2.5	0.623

		Fitted results					
E (eV)	θ (deg)	x_1	x_2	f	g	m	rms error
			No background correction				
500	135	0.043	0.52	1.20	0.09	1.02	0.00
500	130	0.042	0.47	1.16	0.00	0.87	0.13
500	110	0.038	0.55	1.54	0.00[b]		0.00
1000	130	0.044	0.45	1.03	0.00	1.44	0.48
1000	110	0.048	0.42	1.15	0.00[b]		0.00
			With integral background removal				
500	135	0.038	0.60	1.04	0.01	0.55	0.00
500	130	0.039	0.55	0.89	0.00	0.46	0.32
500	110	0.031	0.59	1.53	0.00[b]		0.00
1000	130	0.036	0.55	0.85	0.00	0.78	0.41
1000	110	0.036	0.52	0.92	0.00[b]		0.00

[a]Calculated ratio of scattering cross sections.
[b]Constrained to this value.

composition from measurements at any scattering angle and incident ion energy for which the ratio of the cross sections, s_{Mo}/s_{Re}, is known.

At higher angle, ψ near 63° in the [110] azimuth, scattering from the second layer contributes. Single scattering from third or deeper layers should not be possible at the chosen scattering angles because of blocking. However, scattering from deeper layers by multiple scattering may contribute at the single-scattering energy. The amount of contributions from third or deeper layers is therefore considered parametrically. To remove various instrumental factors, the intensities at the high incident angle are normalized to that at the lower angle, to give Eqs. (1b) and (1c) for Mo and Re:

$$R_2 = I_{Mo}(\psi=63)/I_{Mo}(\psi=40) = [(1-x_1)+(1-x_2)+m(1-x_b)]/(1-x_1) , \tag{1b}$$

$$R_3 = I_{Re}(\psi=63)/I_{Re}(\psi=40) = (x_1+x_2+mx_b)/x_1 . \tag{1c}$$

In these equations x_2 and $(1-x_2)$ are the Re and Mo compositions, respectively, in the second layer, and m is a non-negative parameter describing the amount of contribution from deeper layers. Layers deeper than the second are assumed to have the bulk Re atom fraction $x_b = 0.25$.

Scattering along the [100] azimuth can also be related to the first- and second-layer compositions, but certain possible complications should be considered. It has been observed that along the [100] azimuth of bcc(001) surfaces, enhanced scattering from second-layer atoms can result from focusing.[12] Computer simulations also suggest that similar type trajectories may result in contributions from third-layer atoms. General equations which parametrically describe the scattering along this azimuth for both Mo and Re can be obtained. Again it is convenient to normalize the intensities to the scattering at grazing angles along the [110] azimuth, to give the following equations:

$$R_4 = I_{Mo}([100])/I_{Mo}([110]) = [(1-x_1)+f(1-x_2)+g(1-x_b)]/(1-x_1) , \tag{1d}$$

$$R_5 = I_{Re}([100])/I_{Re}([110]) = (x_1+fx_2+gx_b)/x_1 . \tag{1e}$$

In these equations, the non-negative parameters f and g describe the relative contributions from second and deeper layers, respectively.

This model of the scattering is somewhat more general than that proposed by Buck, Wheatley, and Marachut.[13] In their model the focusing parameter f is considered but possible scattering from deeper layers is ignored, that is, the parameters g and m are assumed to be zero. Equations (1a)–(1e) contain five unknown parameters (x_1, x_2, f, g, and m) since the ratios of the scattering cross section and x_b are assumed to be known, and therefore have a unique solution. The solution may yield unphysical values for the parameters such as negative values of g or m, or values of x_1 or x_2 outside the range of 0–1.0. The measured ratios R_i each have an associated error and the equations exhibit varying sensitivity to these errors. For these reasons, Eqs. (1a)–(1e) were solved, with constraints upon the parameters, by least-squares minimization of the residuals resulting from subtracting the right side of Eqs. (1a)–(1e) from the measured ratios R_i and weighting these residuals according to the expected uncertainty in R_i. This process allowed checking the model by imposing different constraints upon the parameters, such as fixing $f=1.0$ or fixing g to zero, and determining the effect upon the parameters of interest x_1 and x_2. It should also be noted that the cross-section ratio does not enter into Eqs. (1b)–(1e), so the determination of x_2 is only weakly affected by an uncertainty in this ratio.

It remains to consider the process of extracting a single-scattering intensity from measured ion energy distributions such as those shown in Fig. 1. The background below the peaks and the shifting widths and positions of both the Mo and Re "single-scattering" peaks indicate that inelastic scattering makes a contribution which varies with incident angle. The high backgrounds observed in alkali-ion scattering or in the neutral time-of-flight (TOF) spectrum obtained from inert-gas ions are not generally as prominent in inert-gas ion-scattering spectroscopy because of attenuation of all subsurface scattering by neutralization.[14] At present there is no clear strategy for removing these inelastic effects. We have tried two techniques. The first is to use the count rate at the maximum of the single-scattering peak (multiplied by $\sin\psi$ and corrected for the energy-dependent ESA bandwidth) as the best proportionate measure of the single-scattering intensity. This convenient method is based upon the expectation that the elastic single-scattering component is maximum at the observed peak and has an energy width determined only by the scattering geometry. A second technique was to subtract an integral background (such as is frequently used in photoemission[15]) which is fitted to the distribution. This process is illustrated in Fig. 4.

Using these procedures the intensity ratios R_i were obtained at different incident ion energies and laboratory scattering angles. Results are given in Table I. It was found that for scattering angles below about 110° the Mo and Re peaks began to merge sufficiently to complicate the analysis, which together with instrumental constraints ($\theta < 135°$) limited the range of scattering angles. At lower scattering angles ($\theta < 120°$ depending upon ion energy) second-layer scattering is blocked at all incident angles in the [110] azimuth, so for these conditions R_2 and R_3 are not measured and Eqs. (1b) and (1c) and the m parameter are not used. Measurements made for 2000-eV incident energy were not used because the background below the Re peak at grazing angles was so large compared to the Re peak that reliable estimates of the Re single-scattering intensity could not be obtained.

The measured ratios were obtained after repeated anneals of the clean surface over many days. The absolute

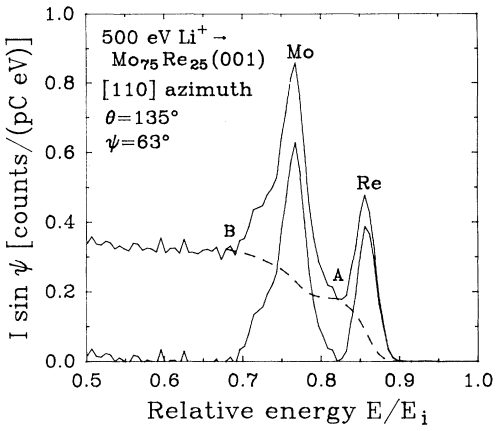

FIG. 4. Energy distributions are shown to demonstrate the background subtraction procedure used. First a background proportional to the integrated intensity of the distribution, integrated from above the Re peak to point *A*, is subtracted. In a second step, the procedure is repeated from point *A* to point *B*. The resulting background and difference are shown. The peak heights of the background subtracted distribution are used for determining intensity ratios.

intensites were found to be very sensitive to adsorption of oxygen and ambient gases, in part because of work-function changes and their effects on Li^+ ion neutralization similar to that observed previously for Mo(001).[16] Certain *ratios* were also sensitive to a buildup of ambient impurities, because of differing effects of adsorbate shadowing and ion neutralization. Care was taken to establish the sensitivity of the ratios to ambient gas exposure and to make sure that the ratios were typical of the clean surface. The ratios were checked at various parts of the sample to ascertain homogeneity, and to eliminate spurious scattering from the W-Re thermocouple which intercepted a fraction of the beam at certain manipulator settings. Estimates of the uncertainties are standard deviations of repeated measurements.

The values of the parameters which minimize the weighted residuals are also shown in Table I both with and without the use of background subtraction, and for different constraints upon f, g, and m. The rms error (defined as the square root of the average squared weighted residual) provides an indication of the fit to the data. For example, a rms error of unity indicates that the average residual is equal to the expected uncertainty. In certain cases exact solutions with physically reasonable parameters are obtained as indicated by a rms error of zero. Each set of scattering conditions provides an independent determination of the parameters. It is seen from examination of Table I that all data sets converge on $x_1 = 0.040 \pm 0.005$. The uncertainty of the scattering cross-section ratio (10%) only slightly increases the uncertainty of this value to ± 0.006. The second-layer composition is less clear with values for x_2 of 0.56 and 0.48 from the background corrected and uncorrected data, respectively.

The data for a scattering angle of 130° typically gave a small negative value for the parameter g, possibly indicating that the third-layer composition is depleted slightly in Mo. Constraining g to be non-negative gave fits with reasonably low rms error with the best fit at $g = 0.0$. Physically this means that scattering from the third layer is not contributing in the [100] azimuth. For a scattering angle of 110° only three measured ratios are obtained but there are four fitting parameters. Based upon the above conclusion, the parameter g was fixed to zero at this scattering angle allowing determination of unique values for the other parameters.

For the results with no background correction, the parameter f is found to be larger than unity, indicative of focused enhancement with a magnitude that depends upon scattering angle and decreases as E_i increases from 500 to 1000 eV. This result is consistent with previous results for Li^+ scattering from Mo(001) where a value of 2.5 is found for f at 500 eV and $\theta = 60°$, which decreases as E_i increases.[12] The nonzero values for m indicate that single scattering can only be partly discriminated from multiple scattering from deeper layers. Background subtraction reduces but does not eliminate this component. The deeper-layer contributions are increased at higher energies.

B. Layer spacing

In principle, it is possible to determine the spacing between the first and second layers by making use of the critical angle of incidence associated with scattering from the second layer in the [110] azimuth. Data shown in Fig. 5 demonstrate how the Mo scattering critical edge varies with incident ion energy. The data are obtained in the manner described above for Fig. 3. It is seen that the S21 edge, caused by shadowing of 2nd-layer Mo by 1st-layer atoms, shifts toward lower angle with increasing incident ion energy as predicted by the decreasing shadow cone size. Similarly, the high-energy cutoff associated with the blocking of second-layer scattering, B21, is seen to shift toward higher angle with increasing ion energy

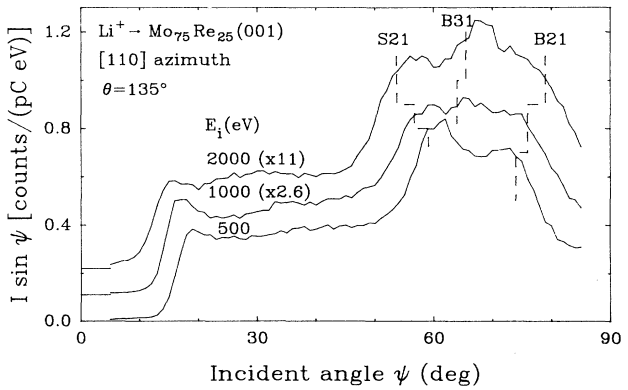

FIG. 5. Scans of the Mo peak heights (corrected for ESA transmission and multiplied by $\sin\psi$) are shown as a function of incident angle in the [110] azimuth for three different incident Li^+ ion energies. The curves for 1000 and 2000 eV are normalized to equal intensity near 40° and offset by an amount indicated by lines at low angle.

because of the decreasing size of the blocking cone.

Using the scattering potentials determined above it is possible to calculate the shadow cone critical angle for the second-layer scattering as a function of interlayer spacing and for different incident ion energies. Results are shown in Fig. 6 for Mo atoms shadowed by first-layer Mo atoms at $\theta=130°$. The first-layer shadowing atom is assumed to be Mo since the first-layer composition is predominantly Mo. The dashed lines indicate the measured critical edge for each ion energy, as determined by the 90% point of the shadowing edge.[8] The Mo single-scattering data indicate that d_{12} is contracted by 6.2%±0.8%. Similarly the Re edge can be used. In this case the critical edge is calculated assuming first-layer Mo atoms shadow second-layer Re atoms. The Re data obtained at three different ion energies yield a contraction of 4.7%±1.4%. Taken together, Mo and Re data indicate a first-layer contraction of about 5.5%±1.6%. The quoted error reflects the magnitude of "random" scatter based on all measurements.

In evaluating the accuracy of this approach it is important to consider the effects of onset of single scattering from deeper layers which could reduce the measured contraction. To test for this possibility measurements were also made at $\theta=135°$. For a scattering angle of 130° it is expected that single scattering from atoms in the third and deeper layers should be blocked by overlying atoms for incident angles near to the shadowing edge, but at $\theta=135°$ blocking should shift the onset of third-layer scattering to still higher incident angles. A possible onset of direct third-layer scattering at B31 is visible in Fig. 5 for the 2000-eV data near $\psi=65°$, which is well separated from the onset of second-layer scattering at lower angles. Measurements made at $\theta=135°$ for both Mo and Re edges for three different energies yielded a 4.1%±0.4% contraction. This determination does not lead to an increase as expected if third-layer single scattering was contributing more at 130° than at 135°. Measurements of both the Mo and Re edges at three energies and for $\theta=130°$ and 135° yield a weighted mean for Δd_{12} of 4.5%±0.4%.

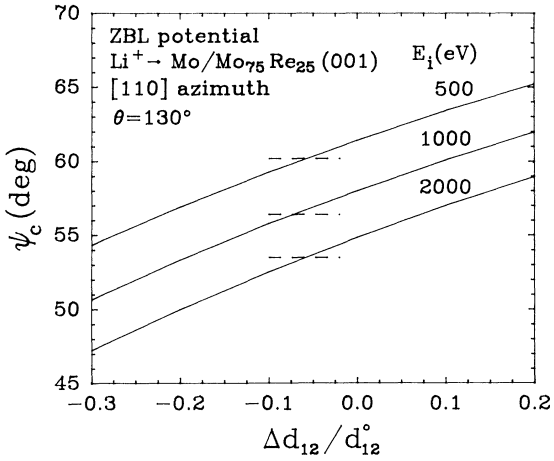

FIG. 6. The calculated critical angle for the onset of scattering from second-layer Mo atoms is shown as a function of the first-second interlayer spacing for three different incident Li^+ ion energies. The measured values of $\psi_{90\%}$ are shown as dashed lines intersecting the appropriate curves.

Another consideration in the accuracy of this determination is the extraction of critical angles from broadened edges. Although there are different rationales, typically the angles associated with 50–90 % of the maximum intensity are used.[8,17] In the determination of the scattering potential from the S11 edge and of the critical angle associated with S21, the 90% point was used. However, it was found that the width of the S21 onset varied with E_i and θ but was broader than the S11 onset, a situation which leads to additional uncertainty. This additional broadening is attributed to the increase of multiple or inelastic (nonsingle) scattering suggested by the nonzero values for m found above. To estimate the sensitivity to this uncertainty, the analysis was repeated using the 50% points both to determine a revised scattering potential from the S11 edge and to use this potential to extract values of d_{12} from the 50% point of the S21 edge. Since the S21 edge is broader than the S11 edge, the predictable effect of using the 50% instead of 90% points is an increase of the resulting contraction. Measurements of both the Mo and Re edges, at three energies and for $\theta=130°$ and 135°, gave a revised value for Δd_{12} of 13.2%±0.4% contracted.

The largest systematic error therefore ultimately results from the width of the S21 edge. At present we cannot decide whether the 50% or the 90% point provides a more accurate estimate, but it seems reasonable that they provide bounds on the true value of Δd_{12}. Therefore the value of d_{12} is reported as 9%±5% contracted.

IV. DISCUSSION

The present results are summarized in Table II and compared with LEED results. It is seen that there is excellent agreement between the LEED and ion-scattering results with respect to the layer compositions, so the oscillatory surface composition profile found by LEED is

TABLE II. Experimental values of layer compositions, x_i, given as Re atom fraction are tabulated for $Mo_{0.75}Re_{0.25}(001)$. The interlayer spacings Δd are also given as deviation in percent from the bulk interlayer spacing of 0.1565 nm.

	Present	LEED[a]
x_1	0.04±0.01	0.04
x_2	0.52±0.05	0.47
x_3		0.24
x_4		0.29
x_5		0.25
x_6		0.25
Δd_{12}	−9±5	−11
Δd_{23}		+5.2
Δd_{34}		−2.7
Δd_{45}		+3.3
Δd_{56}		−2.1
Δd_{67}		+2.4

[a]From Ref. 2.

confirmed for the first two layers in the present study. The ion-scattering results confirm a contraction of the first interlayer spacing, by an amount that agrees with the LEED result within the error estimate of the ion-scattering results. An important difference between the two techniques is that in ion scattering the determination of the layer spacing and compositions is decoupled, so that each parameter is determined separately. In LEED R-factor analysis all parameters affect the I-V curves and cannot be decoupled in the analysis.

The results confirm that the surface composition of this alloy is strongly altered by surface effects. In particular, the first layer is strongly depleted of Re compared to the bulk atom fraction of 0.25. Enrichment of the first layer in Mo is consistent with the predictions of equilibrium surface segregation as described by Abraham and Brundle.[18] Their analysis is based on a consideration of strain and relative bond strengths as the dominant driving factors leading to surface segregation. Strain is characterized by the size ratio σ and the relative bond strengths are determined either by the ratio ε taken from the ratio of enthalpies of sublimation, or γ, taken from surface tension or surface energy measurements. The ratio of radii of Re to Mo is 0.98, as determined from the atomic volumes of bulk Re and Mo. The ratio of the heats of sublimation (of the solids at 0 K) for Re to Mo is 1.18 (Ref. 19) and the ratio of the solid surface energies at 0 K is 1.24.[20] For these values all theories presented in Ref. 18 predict that solute Re will be depleted at the surface of dilute alloys. A more recent critical review by Ossi[21] finds that theories based on the tight-binding approach[22,23] and by models based on surface energy and heat of mixing arguments[24,25] agreed that the solute Re would not segregate preferentially to the surface of a dilute Mo (Re) alloy. Presumably this implies that the solvent Mo will segregate.

As pointed out by Ossi,[21] the predictions of such models fail in a large number of cases either due to shortcomings in the theory or in experimental data. A reason for this is suggested by the present data. The strong oscillations in composition confirmed for the Mo-Re and Pt-Ni systems[1] might now be expected to be a general result for alloys that exhibit strong segregation and have negative enthalpies of formation. This suggests an obvious difficulty in analyzing alloy surfaces by AES which averages over depths of several layers with diminishing contribution from each deeper layer. The advantage of alkali-ion scattering or TOF analysis of neutrals in low-energy ion scattering is the ability to systematically change the extent to which the first and second layers contribute to the scattered signal by variation of the incident angles. Probably the majority of alloy surface measurements performed to date and compared in compilations[18,21] have been analyzed by AES. Also most alloys studied to date have negative enthalpies of formation, since there is a natural bias in that direction. These factors may contribute to difficulties noted by Ossi.

The second layer is enriched in Re, compared to bulk, to a range of $x_2 = 0.52 \pm 0.05$, a large reversal of the first-layer deviation. Such an oscillating composition profile has been generally predicted for alloys with a negative enthalpy of mixing.[25] No experimental measurements of the heat of mixing of Mo-Re alloys could be found to corroborate this prediction. However, from the phase diagram for Mo-Re it is expected that the heat of mixing should be negative but not too large, since ordered compounds form at certain compositions, and since large amounts of Re are soluble in Mo without low-temperature immiscibility. An estimate of the enthalpy of mixing, ΔH_m, can be obtained using the semiempirical theory of Miedema[26] which predicts a value of -2.5 kcal/mol, or using tight-binding theory[27] which predicts a value of about -1 kcal/mol.

Since quantitative values of the first- and second-layer compositions have been determined, it is possible to provide a more quantitative scrutiny of the theoretical predictions. In models based upon ideal configurational entropy the first-layer composition x_1 is given by

$$x_1/(1-x_1) = x_b/(1-x_b)\exp(Q/RT) , \tag{2}$$

where various forms of the energy term Q have been proposed, as summarized by Abraham and Brundle.[18] The model of Miedema,[24] using values found in Table I of that reference and a heat of solution derived from the predicted heat of mixing, gives a value of Q of about -12 kcal/mol. In the model of Williams and Nason,[25]

$$Q = \Delta H_{\text{sub}}(\Delta Z/Z) . \tag{3}$$

Using heats of sublimation of solid Mo and Re at 0 K predicts $Q = -28.0(\Delta Z/Z)$ kcal/mol, where $\Delta Z/Z$ is a ratio describing the reduction of the coordination at the surface to the bulk coordination Z. For a bcc(100) surface, based upon nearest-neighbor interactions alone, $(\Delta Z/Z)$ is 0.5, but the effects of next-nearest-neighbor interactions may be expected to lower this value.

In our experiment the surface was annealed to 2000 K, and then quenched. It is expected that equilibration of the surface by interdiffusion occurs on laboratory time scales only above about $\frac{2}{3}$ of the melting temperature[28] [$T_m = 2800$ K (Ref. 19)], so the resulting surfaces are expected to have a surface composition "frozen" at that for equilibrium temperatures of 1800–2000 K. Using this temperature range and Miedema's estimates of Q, the value of x_1 predicted by Eq. (2) is 0.01–0.015, a bit low compared to the experimental value of 0.04. Using Eq. (3) with $(\Delta Z/Z) = 4/8 = 0.5$ gives a still lower value, but can be made to fit the experiment by choosing $(\Delta Z/Z)$ to be 0.25–0.29 (depending upon temperature), comparable to the coordination of a smooth close-packed surface such as fcc(111).

Calculation of the second-layer composition requires an extension to include deeper layers as was first done by Williams and Nason.[25] Their equations are derived for four layers but can be readily extended to more. These equations were solved using the heat of sublimation difference given above and using $Z\Omega = \Delta H_m/[x_b(1-x_b)]$ with $\Delta H_m = -2.5$ kcal/mol, estimated above. Using values of $(\Delta Z/Z) = 0.5$ based strictly on nearest neighbors for a bcc(100) surface gives strong oscillations, larger than observed. The oscillations also do not damp out in only four layers, possibly indicat-

ing an overestimate of Ω. Using $(\Delta Z/Z)=0.29$ improves the agreement, giving the correct first-layer composition and damping of the oscillations, but the second-layer concentration $x_2=0.31$ is low compared to the experiment.

More detailed methods such as the embedded-atom method (EAM) (Ref. 3) and the tight-binding models[4,5] yield a generalized form of Eq. (2) which can be extended to several layers and in which Q is a function of the composition of the layers. The EAM also explicitly incorporates interatom distance dependence to the pairwise interaction energies and so is dependent upon interlayer spacings. Application of these techniques has reproduced composition oscillations in $Pt_{0.5}Ni_{0.5}(111)$, although not as large as determined by LEED.[3,4]

V. SUMMARY

Ion-scattering measurements support the LEED analysis[2] of the first interlayer spacing and quantitatively confirm that Re segregates away from the first layer and enriches the second layer of the clean, equilibrated $Mo_{0.75}Re_{0.25}(001)$ surface. The combined results present a well-documented alloy surface configuration and provide a good test for theoretical models of alloy surfaces. The observed direction of segregation is in agreement with models based on size mismatch and relative bond energies, but the magnitude of the first-layer segregation is obtained only if the surface coordination is higher than expected based only on the number of nearest neighbors. The second-layer enrichment appears to be larger than predicted by pairwise models.

ACKNOWLEDGMENTS

Research sponsored by the Division of Chemical Sciences, Office of Basic Energy Sciences, U.S. Department of Energy under Contract No. DE-AC05-84OR21400 with Martin Marietta Energy Systems.

[1]Y. Gauthier, R. Baudoing, and J. Jupille, Phys. Rev. B **40**, 1500 (1989), and references therein.
[2]H. L. Davis and B. Dotsch, Bull. Am. Phys. Soc. **36**, 705 (1991).
[3]M. Lundberg, Phys. Rev. B **36**, 4692 (1987).
[4]B. Legrand, G. Treglia, and F. Ducastelle, Phys. Rev. B **41**, 4422 (1990).
[5]S. Gangopadhyay, S. Modak, B. C. Khanra, and J. C. Bertolini, Solid State Commun. **79**, 759 (1991).
[6]S. Deckers, F. H. P. M. Habraken, W. F. van der Weg, A. W. Denier van der Gon, B. Pluis, J. F. van der Veen, and R. Baudoing, Phys. Rev. B **42**, 3253 (1990).
[7]Y. Ku and S. H. Overbury, Surf. Sci. **273**, 341 (1992).
[8]S. H. Overbury and D. R. Huntley, Phys. Rev. B **32**, 6278 (1985).
[9]J. F. Ziegler, J. P. Biersack, and U. Littmark, U.S. DOE Report No. ORNL/CONF 82 013 (1983) (unpublished), p. 88.
[10]D. R. Mullins and S. H. Overbury, Surf. Sci. **193**, 455 (1988).
[11]M. T. Robinson, ORNL Report No. 4556 (1970) (unpublished).
[12]S. H. Overbury, P. C. Stair, and P. A. Agron, Surf. Sci. **125**, 377 (1983).
[13]T. M. Buck, G. H. Wheatley, and L. Marchut, Phys. Rev. Lett. **51**, 43 (1983).
[14]T. M. Buck, G. H. Wheatley, and L. K. Verheij, Surf. Sci. **90**, 635 (1979).
[15]D. A. Shirley, Phys. Rev. B **5**, 4709 (1972).
[16]S. H. Overbury, B. M. DeKoven, and P. C. Stair, Nucl. Instrum. Methods Phys. Res. B **2**, 384 (1984).
[17]M. Aono and R. Souda, Jpn. J. Appl. Phys. **24**, 1249 (1985).
[18]F. F. Abraham and C. R. Brundle, J. Vac. Sci. Technol. **18**, 506 (1981).
[19]R. Hultgren, P. R. Desai, D. T. Hawkins, M. Gleiser, K. K. Kelley, and D. D. Wagman, *Selected Values of the Thermodynamic Properties of Binary Alloys* (American Society for Metals, Metals Park, OH, 1973); *Selected Values of the Thermodynamic Properties of the Elements* (American Society for Metals, Metals Park, OH, 1973).
[20]A. R. Miedema, Z. Metallk. **69**, 287 (1978).
[21]P. M. Ossi, Surf. Sci. **201**, L519 (1988).
[22]S. Mukherjee and L. L. Moran-Lopez, Surf. Sci. **188**, L742 (1987).
[23]J. R. Chelikowsky, Surf. Sci. **139**, L197 (1984).
[24]A.R. Miedema, Z. Metallk. **69**, 455 (1978).
[25]F. L. Williams and D. Nason, Surf. Sci. **45**, 377 (1974).
[26]A. R. Miedema, J. Less-Common Met. **41**, 283 (1975).
[27]D. G. Pettifor, Phys. Rev. Lett. **42**, 846 (1979).
[28]C. T. Campbell, Annu. Rev. Phys. Chem. **41**, 775 (1990).